

Japanese Encephalitis Virus-Induced Peripheral Neuropathy in the Rat Model

Na Zhang

Department of Neurology, General Hospital of Ningxia Medical University, Yinchuan

Yanping Yuan

School of Clinical Medicine, Ningxia Medical University, Yinchuan

Liping Yang

School of Clinical Medicine, Ningxia Medical University, Yinchuan

Guowei Wang

School of Clinical Medicine, Ningxia Medical University, Yinchuan

Huan Yang

School of Clinical Medicine, Ningxia Medical University, Yinchuan

Zhao Wang

School of Clinical Medicine, Ningxia Medical University, Yinchuan

Xiaocong Li

School of Clinical Medicine, Ningxia Medical University, Yinchuan

Liming Yu

School of Clinical Medicine, Ningxia Medical University, Yinchuan

Denger Zhang

School of Clinical Medicine, Ningxia Medical University, Yinchuan

Huanyu Wang

Chinese Center For Disease Control and Prevention

Zhenhai Wang (✉ wangzhenhai1968@163.com)

Neurology Center, General Hospital of Ningxia Medical University, Yinchuan

Research Article

Keywords: Japanese encephalitis virus, Peripheral neuropathy, Ceramides, Matrix metalloproteinase-9, Blood nerve barrier

Posted Date: February 16th, 2022

DOI: <https://doi.org/10.21203/rs.3.rs-1324807/v1>

License: © ⓘ This work is licensed under a Creative Commons Attribution 4.0 International License.

[Read Full License](#)

Abstract

Background: Guillain–Barré Syndrome Associated with Japanese encephalitis virus(JEV) infection,the mechanism of JEV which caused peripheral nerve injury remains unknown.Recently, it has been suggested that an altered sphingolipid metabolism may contribute to the pathogenesis of peripheral neuropathy. In light of the emerging evidence of peripheral nerve injury when JEV infected and the evidence in the pathogenesis of neuroimmunity, we aimed to make a rat model which peripheral nerve injury after JEV infection and investigate relevant damage mechanism.

Methods: We investigated the infected rat with peripheral neuropathy induced by JEV. The rat exhibited behavioral and pathological signs of peripheral nervous injury. The motor function of rats were determined by clinical scoring and tissue examination.Electrophysiological measurements and transmission electron microscopy was used on sciatic nerves to assess peripheral peripheral nervous injury.ELISA were used to evaluate IFN γ , IL-17,ceramide and acid sphingomyelinase level. Immunofluorescence was performed on sciatic nerves to assess the expression and localization of ceramide and matrix metalloproteinase-9.

Results: Japanese encephalitis virus induced peripheral neuropathy in rat,evidenced by the aggravated clinical scores, electrophysiological,transmission electron microscopy,circulating pro-inflammatory cytokines, and histological anomalies, suggesting that demyelination and axonal damage of sciatic nerves. JEV destroyed the tight junction structure of rat's blood nerve barrier and increased ceramide and matrix metalloproteinase-9.

Conclusion:These data suggest that JEV is a potential reason caused peripheral nerve injury in rat model and this model can be used for the investigation of the roles of various cytokines and acid sphingomyelinase,ceramide system in infection-induced peripheral neuropathy. Further investigation of this model could give a better understanding and lead to more effective evidences for JEV infection-associated peripheral neuropathy.

Background

Japanese encephalitis virus (JEV) is a member of the genus Flavivirus, family Flaviviridae, which includes West Nile , Zika and dengue viruses^[1]. It is transmitted by mosquitoes, and is found throughout South and Southeast Asia, the Philippines and Japan to the east and the Australian Torres Strait Islands to the south.The most comprehensive estimate of incidence within the past decade suggests that 69,000 cases of Japanese encephalitis occur every year^[2].

JEV caused Japanese encephalitis when human infected this virus. Clinical features include acute febrile illness, altered mental status, acute psychosis, seizure and acute flaccid paralysis^[3]. The largest outbreak of JEV infection in the period from July through September 2018 occurred in the north of Ningxia, China,we found 161 patients were confirmed as having JEV infection and electromyographic results in 47

patients with JEV infection were consistent with the Guillain– Barré syndrome^[4], limb weakness also can be seen in the rat model infected by JEV^[5]. However, the animal model and the evidence of peripheral nerve damage caused by JEV has not been reported.

Lipids such as cholesterol^[6], ceramide, and glycosphingolipids are major constituent lipid of myelin in peripheral nervous system (PNS) of vertebrates^[7], the high lipid content is the difference between nerve tissue and other tissues. It had found anti-ganglioside antibodies in patients with JEV infection-associated Guillain-Barre Syndrome^[4], and with Zika virus infection^[8]. Ceramide whose availability can be generated in endosomes largely from the hydrolysis of sphingomyelin via acid sphingomyelinase (ASM), is the core structure of all sphingolipids and is a precursor to sphingomyelins, cerebrosides, gangliosides, and sulfatides^[9].

The mechanism of JEV which caused peripheral nerve injury remains unknown. In light of the emerging evidence of peripheral nerve injury when JEV infected and the evidence in the pathogenesis of neuroimmunity, we aimed to determine whether peripheral nerve injury would occur in rats by using the rat sciatic nerve injury model after JEV virus infection. We also studied the changes of ceramide and ASM, peripheral nerve microscopic changes after JEV infection.

Methods

Experimental animals

Albino Wistar rats (12 days old) were procured from Beijing Vital River Laboratory Animal Technology, China. All the animals were housed under controlled conditions as specified by the guidelines under a 12h light-dark cycle at 23 ± 1 °C and 50% relative humidity, with food and water available ad libitum. All experimental procedures were approved by the institutional animal ethical committee of Chinese Center for Disease Control And Prevention (20210429031).

Induction of model and assessment of clinical scores

The nx1887 Japanese encephalitis virus [Chinese Center for Disease Control And Prevention] was injected in the rats (12 days of age) at the midpoint between the two ears of 20 µL of an containing 3×10^6 pfu/ml. For comparison, the classical acute infected model was induced in Wistar rats by infected with JEV nx1887 and rats were injected with phosphate buffered solution (PBS) 20 µL in the rats (12 days of age) at the midpoint between the two ears were used as negative controls. Body motor function evaluation and clinical score were assessed daily from day 0 until 19 days post-infection (dpi). Severity of paresis was graded as follows: 0, normal walking; 1, flaccid tail; 2, Mild to moderate forearm or hindlimb weakness; 3, Severe forearm or hindlimb weakness; 4, Mild to moderate forelimb and hind limb weakness; 5, Severe forelimb and hindlimb weakness; and intermediate scores of 0.5 increments were given to rats with intermediate signs.

Electrophysiology.

Five rats randomly selected from each group were used to measure the sciatic nerve conduction velocity (NCV) at 3, 6, 12 and 19 days after infection. Rats were anesthetized by 10% chloral hydrate injection intraperitoneally (0.3 mL/100 mg). Surgery was performed on the bilateral hind limbs of anesthetized rats. Exposing the sciatic nerve between the biceps femoris and semitendinosus muscles, the nerve was stimulated by a needle electrode at the proximal and distal ends of the nerve respectively. Another needle electrode was inserted into the gastrocnemius muscle to receive the recording. Motor nerve conduction velocity (MNCV) was measured according to the following equation: $MNCV (m/s) = \text{distance between two stimulating electrodes} / \text{time difference between two action potentials}$. The stimulus was digitized and captured with the NDI-093 biological functional system (ShangHai Poseidon Technology Co., Ltd., ShangHai, People's Republic of China). The sciatic nerve was stimulated with constant voltage (0.3 V) square-wave pulses (0.1 ms).

Transmission electron microscope

Sciatic nerves were prefixed with 2.5% glutaraldehyde for 1.5 hours and postfixed with 1% osmic acid for 2 hours. Then, tissues were dehydrated with ethanol-acetone. Pour the pure EMBed 812 into the embedding models and insert the tissues into the pure EMBed 812, and then keep in 37°C oven overnight. 2% uranium acetate saturated alcohol solution avoid light staining for 8 min, rinsed in 70% ethanol for 3 times and then rinsed in ultra pure water for 3 times. 2.6% Lead citrate avoid CO₂ staining for 8 min, and then rinsed with ultra pure water for 3 times. After dried by the filter paper, the cuprum grids were put into the grids board and dried overnight at room temperature. The cuprum grids are observed under HITACHI HT7800/HT7700 Transmission Electron Microscope and take images.

Immunofluorescence assay

Sciatic nerves were fixed in the fixative for more than 24 hours, the tissue was removed from the fixed solution and placed in 15% sucrose solution for 4°C refrigerator dehydration, then transferred into 30% sucrose solution for 4°C refrigerator dehydration. drop OCT embedding agent around the sciatic nerves, put the specimen chuck on the quick freezing table of the frozen section machine for quick freezing and embedding. Frozen section fixed in paraformaldehyde 30 min and then dry in air. and wash three times with PBS (pH 7.4) in a Rocker device, 5 min each. Immerse the slides in EDTA antigen retrieval buffer (pH 8.0) and maintain at a sub-boiling temperature for 8 min, standing for 8 min and then followed by another sub-boiling temperature for 7 min. Slides were then incubated with primary antibodies at 4 °C overnight. The next day, sciatic nerves were washed with PBS and incubated with secondary antibodies diluted 1:300 in 0.1% ovalbumin/PBS for 2 h at 37 °C. Secondary antibodies were Cy3-conjugated goat anti-rabbit IgG, Alexa Fluor 488-conjugated goat anti-rabbit IgG, (WuHan Servicebio Technology CO.LTD), Alexa Fluor 488-conjugated goat anti-mouse IgG, (WuHan Servicebio Technology CO.LTD). After washing, cover slips were mounted using Fluoroshield supplemented with DAPI (WuHan Servicebio

Technology CO.LTD) to visualize the nuclei. We used the following primary antibodies: anti-ceramide mouse IgG (1:100, Sigma-Aldrich C8104), anti-MMP9 rabbit IgG (1:300 Abcam, ab76003), anti-S100-beta rabbit IgG 4G8 clone (1:200 Bioss, 1:100)

Cytokine secretion

Sera from control, JEV infected rats were collected at 6, and 19 dpi. The concentration of IL-17, IFN γ , ASM cytokine and Ceramide were measured in duplicate in undiluted sera using commercial ELISA kits specific were purchased from j&l Biological Industrial Co., Ltd. (Shanghai, China). According to the manufacturer's instructions, results were calculated relative to a standard curve. Cytokine concentrations were presented as picograms per milliliter relative to a standard curve. The theoretical limits of detection were 2000 pg/mL IFN γ , 48pg/mL IL-17, 3200 pg/mL ASM, and 250 pg/mL ceramide.

Statistical analyses

Statistical analysis was performed with GraphPad Prism 8 (GraphPad Software Inc., San Diego, CA, USA). The data are presented as the means \pm SEM. Significant differences between and within multiple groups were examined using ANOVA followed by the Bonferroni correction method. An independent samples t test was used to detect significant differences between two groups. $P < 0.05$ was considered statistically significant.

Results

Effect of JEV on motor function in rats.

To examine the effect of JEV on the motor function of rats, The virus was injected in the rats (12 days of age) at the midpoint between the two ears. All rats developed a disease with an onset at 1dpi, a maximal clinical score of 4 at 1dpi, and recover at 7 dpi. (Fig. 1).

Damaging effect of JEV infection on electrophysiological changes of sciatic nerve in rats

To discover the potential damage effects of JEV on demyelination and axonal degeneration, we performed electrophysiological measurements on five rats with PBS and five rats infected with JEV at 3 dpi (Early stage of acute disease by clinical score), at 6 dpi (Late stage by clinical score of acute disease), at 12 dpi (Early stage by clinical score of disease recovery), and at 19 dpi (Late stage by clinical score of disease recovery). As shown in Fig. 2A, the motor nerve conduction velocity (MNCV) for JEV infected rats and strongly decreased at 3 dpi (20.9 ± 2.41 m/s) and no recovery was observed at 6 or 12 dpi (36.34 ± 4.90 m/s and 36.63 ± 2.63 m/s). It was not significant compared to 19 dpi. (52.74 ± 3.80 m/s) (Fig. 2A). These results suggest that a demyelination of motor fibers existed in JEV infected rats.

Compound muscle action potential (CMAP) latencies and amplitudes were also measured at 3, 6, 12, and 19 dpi. CMAP latency in JEV infected rats was extended at 6 dpi and did not differ significantly from control group at all other time points (Fig. 2B). Maximal CMAP amplitudes in the JEV infected group rats were significantly and strongly reduced at 3dpi and 6 dpi (5.11 ± 0.61 mV and 6.93 ± 0.91 mV, respectively) and were increased at 12 and 19 dpi (11.37 ± 0.82 mV and 14.64 ± 1.27 mV, respectively) when compared to control group (Fig. 2C). These data are indicative of an axonal degeneration and myelin injury.

JEV caused the loss of myelinated fibers of sciatic nerve in rats

To evaluate if JEV induced morphological changes of myelinated fibers in sciatic nerves of infected rats, histological studies were carried out on sciatic nerves from control and JEV infected rats at 6 and 19 dpi. Semi-thin transverse sections of sciatic nerves demonstrated that clinical disability of JEV infected rats were associated with marked reduction of myelinated fibers at 6 dpi and 19dpi when compared to sciatic nerves from the control group, which presented a well-defined structure and uniform myelin sheath thickness (Fig. 3A–D). Electron microscopy showed that the myelin lamella was loose, the structure was damaged at 3dpi (Fig. 5A,C).

JEV increased the serum levels of IL-17, IFN- γ pro-inflammatory cytokines and ASM and ceramide in infected rats

We also examined whether the JEV in increasing inflammatory cell infiltration in peripheral nervous system (PNS) and causes clinical symptoms of rat were accompanied by a raise level of peripheral pro-inflammatory cytokines and Acid sphingomyelinase/ceramide system. IL-17, IFN γ , ASM, and ceramide levels were measured in the sera of control, JEV infected rats collected at 6 and 19 dpi. JEV infected rat IL-17, IFN γ , ASM and ceramide levels were increased when they are at 6dpi, IL-17 has been maintained at a high level at 19dpi, and IFN- γ pro-inflammatory cytokine levels, ASM and ceramide levels in the JEV infected group was reduced at 19 dpi. There were no significant differences for IFN- γ , ASM and ceramide levels at 19dpi between the two groups (Fig. 4A–D).

JEV destroyed the tight junction structure of rat's BNB

The architectures of tight junctions in the distal sciatic nerve segments were detected by transmission electron microscopy. Myelin sheaths were observed in normal sciatic nerve segments (Figure 5A). Moreover, morphological images showed that tight junctions were observed in the outer mesaxons of myelinated axons (Figure 5B). In JEV infected rat sciatic nerve, we found that the myelin sheath was collapsed and dissolved (Figure 5C). It was observed that the part of the axonal degeneration and dissolved at 3 days after JEV infected rat (Figure 5C). Comparing with normal nerves (Figure 5B), the structure of tight junctions in infected nerve segments was less compact with larger cellular distances (Figure 5D).

JEV induced the increasion of ceramide and MMP9 in rat sciatic nerve

The results of the immunofluorescent study are presented in Figure 6. On transverse sections of the sciatic nerve of control rats (n = 3), the immunofluorescent of ceramide had a diffuse signal in the endoneurium areas and the perineurium areas (Figure 6A). JEV led to a significant increase in ceramide immunoreactivity at 6dpi (Figure 6B). The total fluorescence intensity was enhanced in the JEV infected sciatic nerve at 6dpi (n = 3), (p < 0.001). The most intense labeling was located in the perineurium region. Increased fluorescence was determined both in clusters near the endoneurium and in the perineurium. Compared with the control group of ceramide at 19 dpi (Figure 6C),JEV also led to a significant increase in ceramide immunoreactivity at 19dpi (Figure 6D).The total fluorescence intensity, was enhanced in the JEV infected sciatic nerve at 19dpi (n = 3), (p < 0.01). The most intense labeling was located in the perineurium region. Increased fluorescence was determined both in clusters near the endoneurium and in the perineurium.

Ceramide might play a mediatory role in both matrix degradation and apoptosis in processes [10],ceramide induced matrix metalloproteinase-1[MMP1][matrix metalloproteinase-9[MMP9] expression [11,39].Therefore, we first determined whether JEV induced MMP-9 expression was mediated through ceramide in rats. As shown by the immunofluorescent experiments in transverse sections of the sciatic nerve,the immunofluorescent of MMP9 had highlight signal around blood vessel areas in control group at 6dpi(Figure 7A).JEV led to a significant expression in MMP-9 immunoreactivity at 6dpi in sciatic nerve,MMP9 had a diffuse signal in the nerve (Figure 7B) . The total fluorescence intensity was enhanced in the JEV infected sciatic nerve at 6dpi (n = 3), (p < 0.001). And the control group of MMP9 at 19 dpi (Figure 7C) ,JEV infected rats had increased in MMP9 immunoreactivity at 19dpi (Figure 7D).The total fluorescence intensity, was enhanced in the JEV infected sciatic nerve at 19dpi (n = 3), (p < 0.001).

Discussion

JEV is a member of the flavivirus which can cause encephalitis, cognitive impairment, seizure disorders, and paralysis [12].Zika virus(ZIKV) [13,14]and Dengue virus [15]can induce Guillain-Barré syndrome (GBS),West Nile virus(WNV)caused acute flaccid paralysis [16].And we found JEV infection is also associated with Guillain-Barré Syndrome [4].GBS is a kinds of neuroinflammatory diseases of the peripheral nerves and nerve roots that is usually triggered by infections [17]. GBS is a rare, but potentially fatal, immune-mediated disease of the peripheral nerves and nerve roots that is usually triggered by infections [18,19]. In ZIKA mouse model, dorsal root ganglion(DRG)was also found to support viral infection [20].The mechanism of how JEV damages peripheral nerves is unknown,we created an JEV infected rat model to study peripheral nerve damage.In our study ,we found CMAP amplitudes in the JEV infected group rats were significantly and strongly reduced at 3dpi and 6 dpi and were increased at 12 and 19 dpi ,the motor nerve conduction velocity (MNCV) for JEV infected rats and strongly decreased at 3 dpi and no recovery was observed at 6 or 12 dpi ,and it was not significant compared to 19 dpi,CAMP

latency was extended only in the 6dpi. The nature of the cellular and structural injury in the nerve defies imaging in most scenarios, and electrodiagnostic testing is currently the most sensitive and specific method to evaluate peripheral nerve injury (PNI). Nerve conduction study (NCS) determines nerve conduction velocities to help evaluate axonal degeneration from demyelinating disorders^[21]. Electron microscopy showed that the myelin lamella was loose, the structure was damaged, and the bulge was myelin ball at 3dpi and 19dpi. Semi-thin transverse sections of sciatic nerves demonstrated that clinical disability of JEV infected rats were associated with marked reduction of myelinated fibers at 6 dpi and 19dpi when compared to control group's sciatic nerves.

JEV is one of enveloped RNA viruses which can cause human severe central system infection diseases, the life cycle of this virus is critically dependent on host lipid biosynthesis^[22], pivotal biological function of lipid metabolism during JEV infection^[23]. From viral binding and entry, infection by these viruses leads to reorganization of cellular membranes and lipid metabolism to support the production of new viral particles^[24,25]. Recent work has focused on defining the involvement of specific lipid classes in above process in hopes of identifying potential therapeutic targets for the treatment or prevention of disease. ASM is essential for proper fusion of late phagosomes with lysosomes, which is crucial for efficient transfer of lysosomal antibacterial hydrolases into phagosomes^[26] and ASM activation is critically involved in the activation of endothelial inflammasomes and subsequent oxidative signaling by lipid raft-associated redox platforms, release of cytokines, activation of stress kinases, and altering tight junctions in epithelial cells^[27]. In our study, we found ASM was increased in serum at 6dpi and returned to normal level at 19dpi. Switching the current pH status by two orders of magnitudes, the ASM enzyme is capable of rapid and transient ceramide formation upon activation^[28]. Ceramides are bioactive sphingolipids that support the structure of the plasma membrane and mediate numerous cell-signaling events in eukaryotic cells^[29,30]. Ceramides act as second messengers transduced cellular signals and it has attracted substantial attention in several fields of Biology^[31,32], they are also especially important in the induction of apoptosis^[33]. We found ceramide was increased both 6dpi and 19dpi in sciatic nerve, and it increased in serum at 6dpi. Tani found ceramide plays crucial roles in not only entry but also egress processes of JEV^[31], and ceramide a significant increase in the WNV infected cells was noticed^[34]. Thus, an increase in ceramide is observed during neuroinflammatory disease^[35], and highlights the potential of sphingolipids as a new therapeutic and diagnostic target for neuroinflammatory diseases.

We found JEV can damage peripheral nerve's Blood Nerve Barrier (BNB). The exchange of solutes between the blood and the nerve tissue is mediated by specific and high selective barriers in order to ensure the integrity of the different compartments of the nervous system^[36]. Different diseases can lead to or be accompanied by nerve barrier disruption; impairment of nerve barriers in turn worsens pathology^[37]. Ceramide can cause vascular endothelial cell damage and vascular barrier damage^[38] and make MMP9 increased^[39], which opens the endoneurium^[37]. Breaking the diffusion barrier (such as blood nerve barrier) may increase the contact among spinal root and peripheral nerve and macromolecules^[40]. In this study, it was also found that ceramide and MMP9 increased in the sciatic

nerve of JEV infected rats. The structure of tight junctions in infected nerve segments was less compact with larger cellular distances by transmission electron microscopy. It provides evidence for JEV to damage the peripheral nerve.

In conclusion, we showed that the motor nerve conduction velocity of sciatic nerve decreased, the latency prolonged and the amplitude decreased in JEV injected rats, especially on the 6dpi, we know JEV can cause neuroinflammation, including immune cell infiltration and neuronal degeneration, which has been known as a key factor of JEV pathogenesis in human^[41]. To date, no specific treatment has been approved to overcome JE, indicating a need for the development of novel therapies^[42]. We showed that ceramide has gone up in host and the MMP9 destroyed the tight junction of endothelial cells also increased. The structure of tight junctions in infected nerve segments was less compact with larger cellular distances by transmission electron microscopy. These findings demonstrate that JEV can cause peripheral nerve damage and the evidence of BNB damage in hopes of identifying potential therapeutic targets for the treatment or prevention of disease.

Conclusion

These data suggest that a rat model of peripheral nerve injury with JEV infection is proposed and JEV associated that can be used for the investigation of the roles of various cytokines and sphingolipids in infection-induced peripheral neuropathy. JEV activates the acid sphingomyelinase/ceramide system and damages peripheral nerve's Blood Nerve Barrier. Further investigation of this model could give a better understanding, and lead to more effective treatments for JEV infection-associated peripheral neuropathy.

Abbreviations

JEV Japanese encephalitis virus

WNV West Nile virus

ZIKV Zika virus

GBS Guillain-Barré syndrome

MNCV Motor nerve conduction velocity

CMAP Compound muscle action potential

BNB Blood Nerve Barrier

MMP9 Matrix metalloproteinase-9

MMP1 Matrix metalloproteinase-1

ASM Acid sphingomyelinase

PNI Peripheral nerve injure

NCS Nerve conduction study

PNS Peripheral nervous system

DRG Dorsal root ganglion

Declarations

Authors' contributions

Zhenhai Wang and Huanyu Wang provided the experimental design; Na Zhang wrote the draft of the manuscript; Huan Yang, Na Zhang,Zhao Wang,Liming Yu performed the experiments; Yanping Yuan and Liping Yang analyzed the data; Guowei Wang,Xiaocong Li,Denger Zhang prepared all figures, Na Zhang, Yanping Yuan , Liping Yang wrote, reviewed and edited the manuscript.The author(s) read and approved the final manuscript.

Funding

This study was supported by grants from the Science and Technology Key Research Program of Ningxia, China (2019BCG01003, to Dr. Zhenhai Wang), and the National Natural Science Foundation of China (81960233, to Dr. Zhenhai Wang).

Availability of data and materials

Data can be made available from the corresponding author upon reasonable request and after approval from the ethics review board at the Ningxia Medical University

Ethics approval and consent to participate

This study was approved by the ethics committee at the Chinese Center for Disease Control And Prevention (20210429031).

Consent for publication

Not applicable.

Competing interests

The authors declares that there are no conflict of interest exists in the paper.

References

- [1] Okamoto T, Suzuki T, Kusakabe S, Tokunaga M, Hirano J, Miyata Y, Matsuura Y. Regulation of Apoptosis during Flavivirus Infection. *Viruses*. 2017 Aug 28;9(9):243. doi: 10.3390/v9090243.
- [2] Turtle L, Solomon T. Japanese encephalitis - the prospects for new treatments. *Nat Rev Neurol*. 2018 Apr 26;14(5):298-313.
- [3] Keng LT, Chang LY. Japanese encephalitis. *CMAJ*. 2018 May 28;190(21):E657. doi: 10.1503/cmaj.171341.
- [4] Wang G, Li H, Yang X, Guo T, Wang L, Zhao Z, Sun H, Hou X, Ding X, Dou C, Ma Q, Yang X, Wang Y, Wang Z, Wang L, Liu J, Wang Z, Wang H, Xie P. Guillain-Barré Syndrome Associated with JEV Infection. *N Engl J Med*. 2020 Sep 17;383(12):1188-1190. doi: 10.1056/NEJMc1916977.
- [5] Yanbing D, Lixia H, Jun C, Song H, Fahu Y, Jinwen T. Corilagin Attenuates the Parkinsonism in Japanese Encephalitis Virus Induced Parkinsonism. *Transl Neurosci*. 2018 Jul 18;9:13-16. doi: 10.1515/tnsci-2018-0003.
- [6] Saher G, Brügger B, Lappe-Siefke C, Möbius W, Tozawa R, Wehr MC, Wieland F, Ishibashi S, Nave KA. High cholesterol level is essential for myelin membrane growth. *Nat Neurosci*. 2005 Apr;8(4):468-75. doi: 10.1038/nn1426. Epub 2005 Mar 27.
- [7] Posor Y, Haucke V. A Golgi-associated lipid kinase controls peripheral nerve myelination. *Proc Natl Acad Sci U S A*. 2020 Dec 8;117(49):30873-30875. doi: 10.1073/pnas.2021130117. Epub 2020 Nov 13.
- [8] Rivera-Correa J, de Siqueira IC, Mota S, do Rosário MS, Pereira de Jesus PA, Alcantara LCJ, Ernst JD, Rodriguez A. Anti-ganglioside antibodies in patients with Zika virus infection-associated Guillain-Barré Syndrome in Brazil. *PLoS Negl Trop Dis*. 2019 Sep 17;13(9):e0007695. doi: 10.1371/journal.pntd.0007695.
- [9] Tobias F, Pathmasiri KC, Cologna SM. Mass spectrometry imaging reveals ganglioside and ceramide localization patterns during cerebellar degeneration in the *Npc1*^{-/-} mouse model. *Anal Bioanal Chem*. 2019 Sep;411(22):5659-5668. doi: 10.1007/s00216-019-01989-7. Epub 2019 Jun 29.
- [10] Sabatini M, Rolland G, Léonce S, Thomas M, Lesur C, Pérez V, de Nanteuil G, Bonnet J. Effects of ceramide on apoptosis, proteoglycan degradation, and matrix metalloproteinase expression in rabbit articular cartilage. *Biochem Biophys Res Commun*. 2000 Jan 7;267(1):438-44. doi: 10.1006/bbrc.1999.1983.
- [11] Bauer J, Liebisch G, Hofmann C, Huy C, Schmitz G, Obermeier F, Bock J. Lipid alterations in experimental murine colitis: role of ceramide and imipramine for matrix metalloproteinase-1 expression. *PLoS One*. 2009 Sep 29;4(9):e7197. doi: 10.1371/journal.pone.0007197.
- [12] Pierson TC, Diamond MS. The continued threat of emerging flaviviruses. *Nat Microbiol*. 2020 Jun;5(6):796-812. doi: 10.1038/s41564-020-0714-0. Epub 2020 May 4.

- [13] Katz I, Gilburd B, Shovman O. Zika autoimmunity and Guillain-Barré syndrome. *Curr Opin Rheumatol*. 2019 Sep;31(5):484-487. doi: 10.1097/BOR.0000000000000629.
- [14] Cao-Lormeau VM, Blake A, Mons S, Lastère S, Roche C, Vanhomwegen J, Dub T, Baudouin L, Teissier A, Larre P, Vial AL, Decam C, Choumet V, Halstead SK, Willison HJ, Musset L, Manuguerra JC, Despres P, Fournier E, Mallet HP, Musso D, Fontanet A, Neil J, Ghawché F. Guillain-Barré Syndrome outbreak associated with Zika virus infection in French Polynesia: a case-control study. *Lancet*. 2016 Apr 9;387(10027):1531-1539. doi: 10.1016/S0140-6736(16)00562-6. Epub 2016 Mar 2.
- [15] Rodríguez Y, Rojas M, Pacheco Y, Acosta-Ampudia Y, Ramírez-Santana C, Monsalve DM, Gershwin ME, Anaya JM. Guillain-Barré syndrome, transverse myelitis and infectious diseases. *Cell Mol Immunol*. 2018 Jun;15(6):547-562. doi: 10.1038/cmi.2017.142. Epub 2018 Jan 29.
- [16] Sejvar JJ, Leis AA, Stokic DS, Van Gerpen JA, Marfin AA, Webb R, Haddad MB, Tierney BC, Slavinski SA, Polk JL, Dostrow V, Winkelmann M, Petersen LR. Acute flaccid paralysis and West Nile virus infection. *Emerg Infect Dis*. 2003 Jul;9(7):788-93. doi: 10.3201/eid0907.030129.
- [17] Toscano G, Palmerini F, Ravaglia S, Ruiz L, Invernizzi P, Cuzzoni MG, Franciotta D, Baldanti F, Daturi R, Postorino P, Cavallini A, Micieli G. Guillain-Barré Syndrome Associated with SARS-CoV-2. *N Engl J Med*. 2020 Jun 25;382(26):2574-2576. doi: 10.1056/NEJMc2009191. Epub 2020 Apr 17.
- [18] Leonhard SE, Mandarakas MR, Gondim FAA, Bateman K, Ferreira MLB, Cornblath DR, van Doorn PA, Dourado ME, Hughes RAC, Islam B, Kusunoki S, Pardo CA, Reisin R, Sejvar JJ, Shahrizaila N, Soares C, Umapathi T, Wang Y, Yiu EM, Willison HJ, Jacobs BC. Diagnosis and management of Guillain-Barré syndrome in ten steps. *Nat Rev Neurol*. 2019 Nov;15(11):671-683. doi: 10.1038/s41582-019-0250-9. Epub 2019 Sep 20.
- [19] Willison HJ, Jacobs BC, van Doorn PA. Guillain-Barré syndrome. *Lancet*. 2016 Aug 13;388(10045):717-27. doi: 10.1016/S0140-6736(16)00339-1. Epub 2016 Mar 2.
- [20] Fu TL, Ong KC, Tan SH, Wong KT. Japanese Encephalitis Virus Infects the Thalamus Early Followed by Sensory-Associated Cortex and Other Parts of the Central and Peripheral Nervous Systems. *J Neuropathol Exp Neurol*. 2019 Dec 1;78(12):1160-1170. doi: 10.1093/jnen/nlz103.
- [21] Modrak M, Talukder MAH, Gurgenshvili K, Noble M, Elfar JC. Peripheral nerve injury and myelination: Potential therapeutic strategies. *J Neurosci Res*. 2020 May;98(5):780-795. doi: 10.1002/jnr.24538. Epub 2019 Oct 13.
- [22] Farfan-Morales CN, Cordero-Rivera CD, Reyes-Ruiz JM, Hurtado-Monzón AM, Osuna-Ramos JF, González-González AM, De Jesús-González LA, Palacios-Rápalo SN, Del Ángel RM. Anti-flavivirus Properties of Lipid-Lowering Drugs. *Front Physiol*. 2021 Oct 7;12:749770. doi: 10.3389/fphys.2021.749770.

- [23] Li M, Yang J, Ye C, Bian P, Yang X, Zhang H, Luo C, Xue Z, Lei Y, Lian J. Integrated Metabolomics and Transcriptomics Analyses Reveal Metabolic Landscape in Neuronal Cells during JEV Infection. *Viol Sin.* 2021 Sep 24. doi: 10.1007/s12250-021-00445-0. Epub ahead of print. Erratum in: *Viol Sin.* 2021 Nov 24.
- [24] Yager EJ, Konan KV. Sphingolipids as Potential Therapeutic Targets against Enveloped Human RNA Viruses. *Viruses.* 2019 Oct 1;11(10):912. doi: 10.3390/v11100912.
- [25] Beckmann N, Becker KA. Ceramide and Related Molecules in Viral Infections. *Int J Mol Sci.* 2021 May 26;22(11):5676. doi: 10.3390/ijms22115676.
- [26] Schramm M, Herz J, Haas A, Krönke M, Utermöhlen O. Acid sphingomyelinase is required for efficient phago-lysosomal fusion. *Cell Microbiol.* 2008 Sep;10(9):1839-53. doi: 10.1111/j.1462-5822.2008.01169.x. Epub 2008 May 13.
- [27] Becker KA, Fahsel B, Kemper H, Mayeres J, Li C, Wilker B, Keitsch S, Soddemann M, Sehl C, Kohnen M, Edwards MJ, Grassmé H, Caldwell CC, Seitz A, Fraunholz M, Gulbins E. Staphylococcus aureus Alpha-Toxin Disrupts Endothelial-Cell Tight Junctions via Acid Sphingomyelinase and Ceramide. *Infect Immun.* 2017 Dec 19;86(1):e00606-17. doi: 10.1128/IAI.00606-17. PMID: 29084896.
- [28] Chung HY, Claus RA. Keep Your Friends Close, but Your Enemies Closer: Role of Acid Sphingomyelinase During Infection and Host Response. *Front Med (Lausanne).* 2021 Jan 21;7:616500. doi: 10.3389/fmed.2020.616500.
- [29] Albeituni S, Stiban J. Roles of Ceramides and Other Sphingolipids in Immune Cell Function and Inflammation. *Adv Exp Med Biol.* 2019;1161:169-191. doi: 10.1007/978-3-030-21735-8_15.
- [30] de Wit NM, den Hoedt S, Martinez-Martinez P, Rozemuller AJ, Mulder MT, de Vries HE. Astrocytic ceramide as possible indicator of neuroinflammation. *J Neuroinflammation.* 2019 Feb 25;16(1):48. doi: 10.1186/s12974-019-1436-1.
- [31] Tani H, Shiokawa M, Kaname Y, Kambara H, Mori Y, Abe T, Moriishi K, Matsuura Y. Involvement of ceramide in the propagation of Japanese encephalitis virus. *J Virol.* 2010 Mar;84(6):2798-807. doi: 10.1128/JVI.02499-09. Epub 2010 Jan 6.
- [32] Kurz J, Parnham MJ, Geisslinger G, Schiffmann S. Ceramides as Novel Disease Biomarkers. *Trends Mol Med.* 2019 Jan;25(1):20-32. doi: 10.1016/j.molmed.2018.10.009. Epub 2018 Nov 23.
- [33] Maceyka M, Spiegel S. Sphingolipid metabolites in inflammatory disease. *Nature.* 2014 Jun 5;510(7503):58-67. doi: 10.1038/nature13475.
- [34] Martín-Acebes MA, Merino-Ramos T, Blázquez AB, Casas J, Escribano-Romero E, Sobrino F, Saiz JC. The composition of West Nile virus lipid envelope unveils a role of sphingolipid metabolism in flavivirus biogenesis. *J Virol.* 2014 Oct;88(20):12041-54. doi: 10.1128/JVI.02061-14. Epub 2014 Aug 13.

- [35] Lee JY, Jin HK, Bae JS. Sphingolipids in neuroinflammation: a potential target for diagnosis and therapy. *BMB Rep.* 2020 Jan;53(1):28-34. doi: 10.5483/BMBRep.2020.53.1.278.
- [36] Maiuolo J, Gliozzi M, Musolino V, Carresi C, Nucera S, Macrì R, Scicchitano M, Bosco F, Scarano F, Ruga S, Zito MC, Oppedisano F, Mollace R, Paone S, Palma E, Muscoli C, Mollace V. The Role of Endothelial Dysfunction in Peripheral Blood Nerve Barrier: Molecular Mechanisms and Pathophysiological Implications. *Int J Mol Sci.* 2019 Jun 20;20(12):3022. doi: 10.3390/ijms20123022.
- [37] Reinhold AK, Rittner HL. Characteristics of the nerve barrier and the blood dorsal root ganglion barrier in health and disease. *Exp Neurol.* 2020 May;327:113244. doi: 10.1016/j.expneurol.2020.113244. Epub 2020 Feb 10.
- [38] Jernigan PL, Makley AT, Hoehn RS, Edwards MJ, Pritts TA. The role of sphingolipids in endothelial barrier function. *Biol Chem.* 2015 Jun;396(6-7):681-91. doi: 10.1515/hsz-2014-0305.
- [39] Xuan L, Han F, Gong L, Lv Y, Wan Z, Liu H, Ren L, Yang S, Zhang W, Li T, Tan C, Liu L. Ceramide induces MMP-9 expression through JAK2/STAT3 pathway in airway epithelium. *Lipids Health Dis.* 2020 Aug 24;19(1):196. doi: 10.1186/s12944-020-01373-w.
- [40] Stubbs EB Jr. Targeting the blood-nerve barrier for the management of immune-mediated peripheral neuropathies. *Exp Neurol.* 2020 Sep;331:113385. doi: 10.1016/j.expneurol.2020.113385. Epub 2020 Jun 17.
- [41] Zheng B, Wang X, Liu Y, Li Y, Long S, Gu C, Ye J, Xie S, Cao S. Japanese Encephalitis Virus infection induces inflammation of swine testis through RIG-I-NF- κ B signaling pathway. *Vet Microbiol.* 2019 Nov;238:108430. doi: 10.1016/j.vetmic.2019.108430. Epub 2019 Sep 28.
- [42] Ashraf U, Ding Z, Deng S, Ye J, Cao S, Chen Z. Pathogenicity and virulence of Japanese encephalitis virus: Neuroinflammation and neuronal cell damage. *Virulence.* 2021 Dec;12(1):968-980. doi: 10.1080/21505594.2021.1899674.

Figures

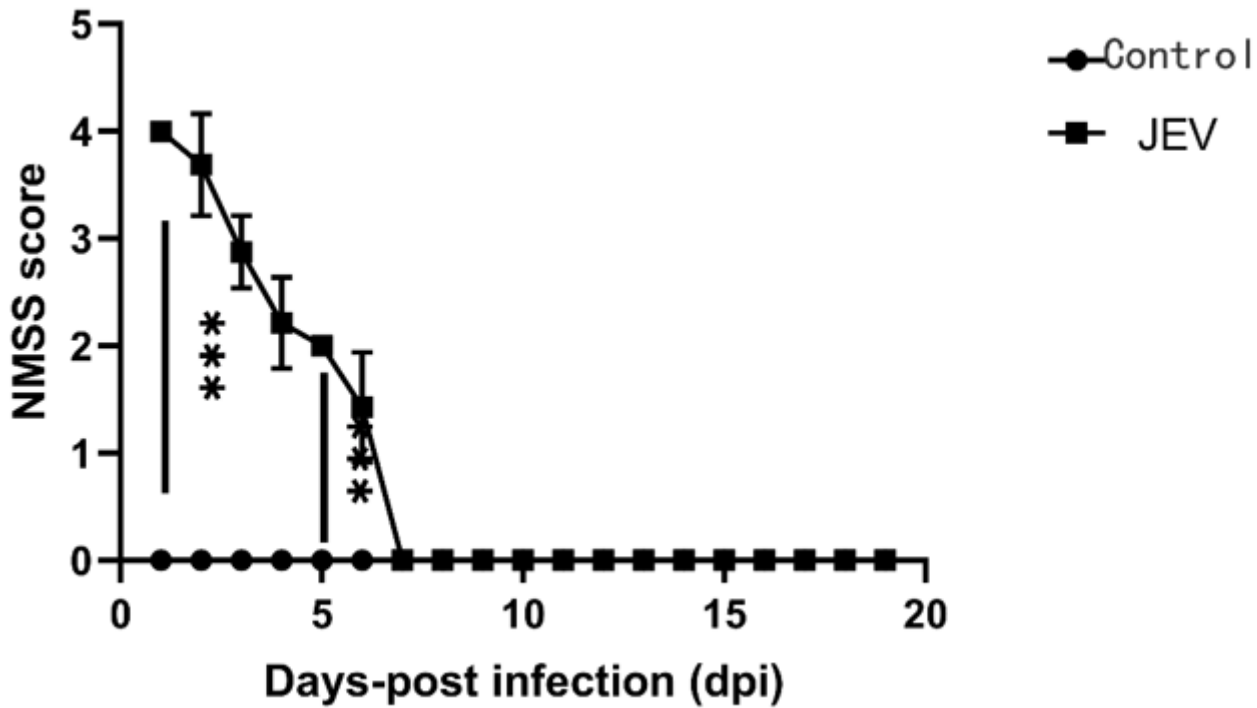


Figure 1

The effect of JEV on the clinical course . Clinical score values were measured rats in control group and JEV infected group. Injections of JEV and control group were administrated intracranially from 1 to 19 days post infection(dpi). Mean values, SEM, and p values are indicated. *p < 0.05; **p < 0.01; ***p < 0.001; ****p < 0.0001. For control group, n = 24 from 0 to 3 days post-infection (dpi), n = 18 from 4 to 6dpi, n = 12 from 7 to 12 dpi ,and n = 6 from 13to 19 dpi; for JEV infected group, n = 24 from 0 to 3 dpi, n =18 from 4 to 6 dpi, n = 12 from 7 to 12 dpi ,and n = 6 from 13 to 19 dpi. n, number of rats.

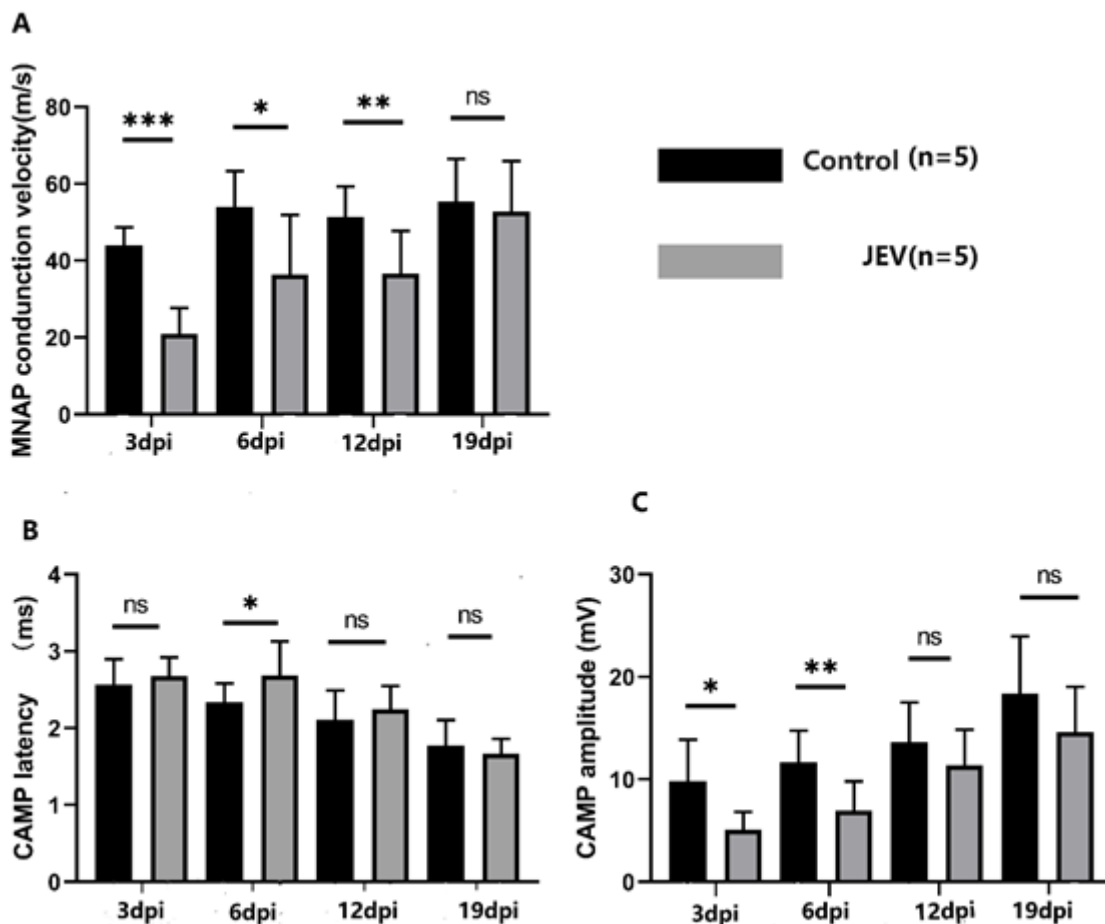


Figure 2

Electrophysiological changes in rats infected JEV at 3, 6, 12, and 19 dpi. A Motor nerve action potential (MNAP) conduction velocity of the sciatic nerve. B Sciatic motor nerve distal CMAP latency. C CMAP amplitudes obtained after proximal stimulation of the sciatic nerve. Mean values, SEM, and p values are indicated. *p values refer to difference between JEV group and the control group at the same dpi *p < 0.05; **p < 0.01; ***p < 0.001; ****p < 0.0001. n = 5 rats/group. n, number of rats.

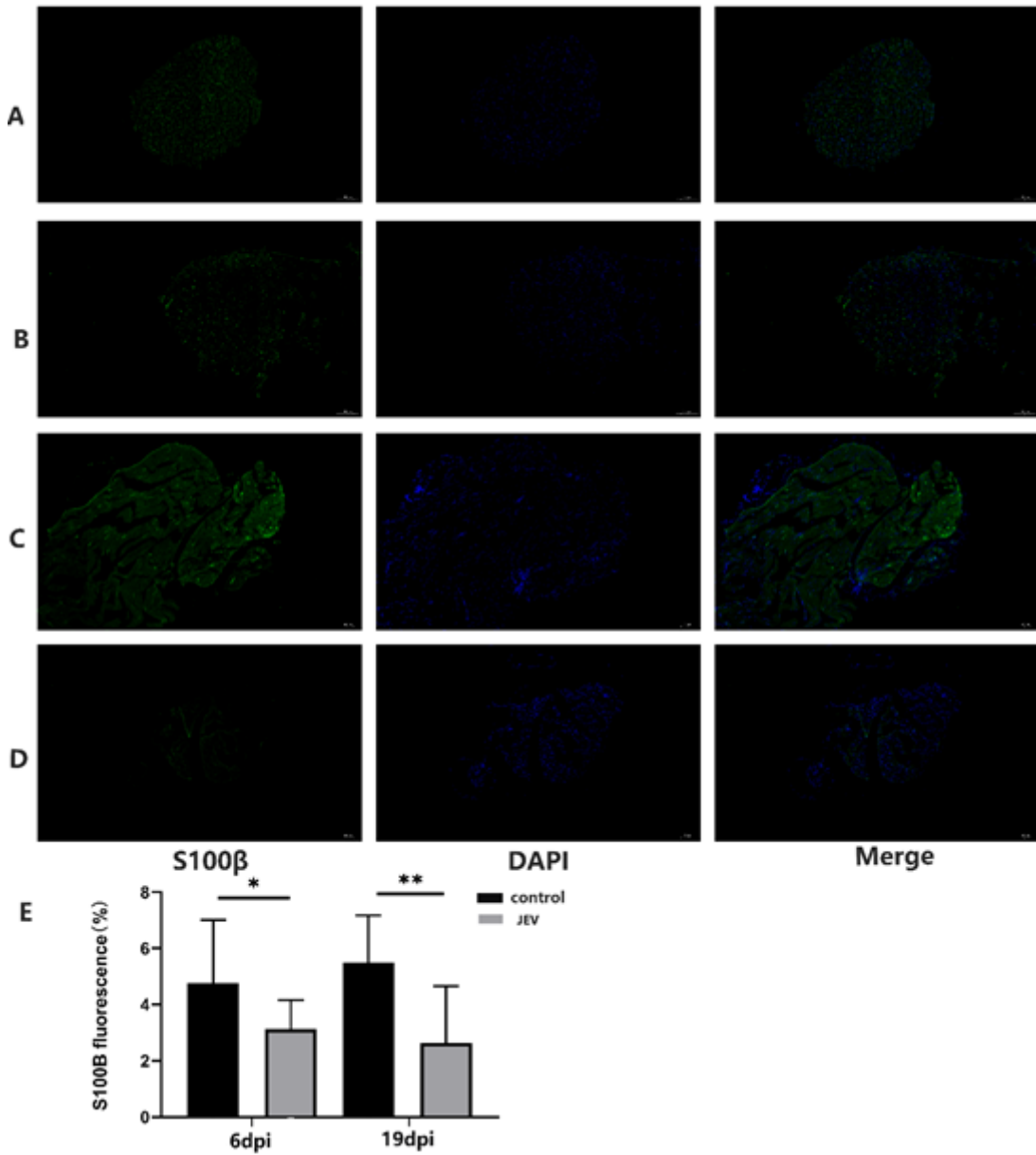


Figure 3

Demyelination of sciatic nerve in rats induced by JEV. Representative semi-thin cross sections of sciatic nerves from control stained with S100 β at 6dpi(A) and 19dpi(C) and JEV infected rats' sciatic nerves from control stained with S100 β at 6dpi(B) and 19dpi(D).Number of average fluorescence area with S100 β which represents myelinated fibers e.Scale bar-100 μ m,mean values, SEM, and p values are indicated. * $p < 0.05$; ** $p < 0.01$. $n=3$, n , number of rats. Representative frozen cross sections of sciatic nerves taken from the two groups of rats and labeled with anti-s100 β antibody for myelin at 6 dpi and 19 dpi.

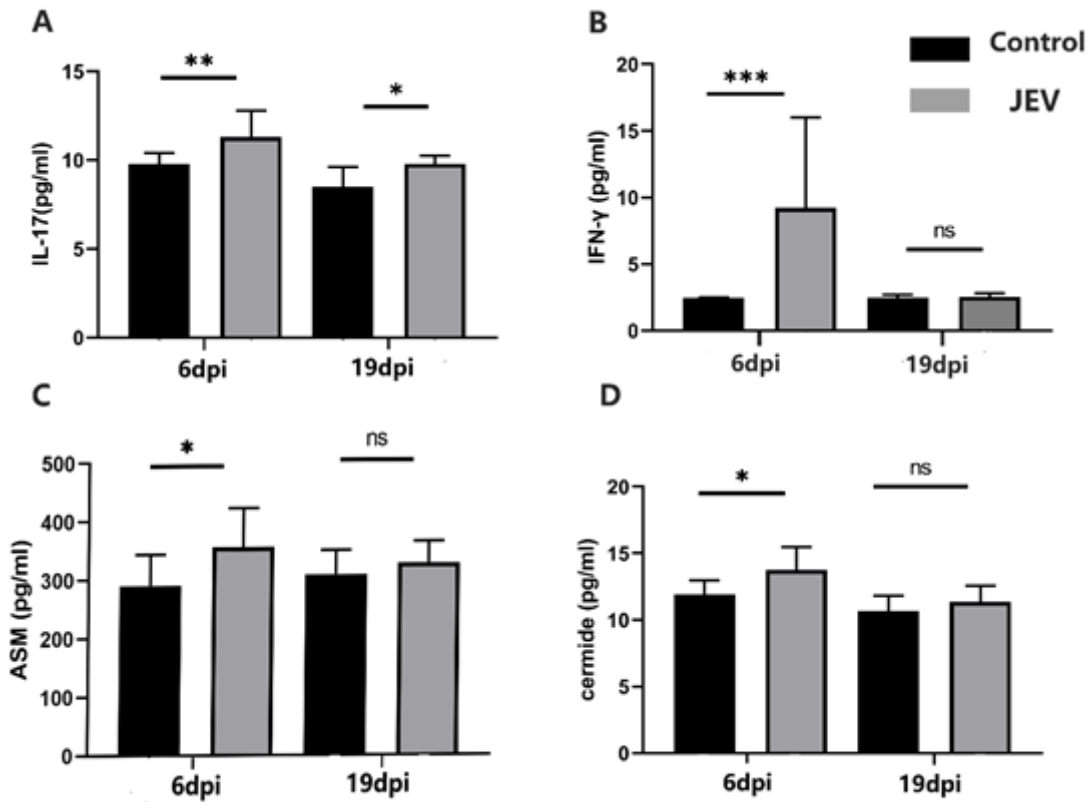


Figure 4

Effect of JEV on serum IL-17, IFN-γ cytokine, ASM and ceramide . Cytokine levels were evaluated at different stages of the disease (6, and 19 dpi) in the serum collected from control rats that received PBS alone or from infected rats that were infected with JEV. (A) IL-17 level (B) IFN-γ level (C) ASM level (D) Ceramide level was evaluated by ELISA. Mean values, SEM, and p values are indicated. *p < 0.05; **p < 0.01; ***p < 0.001; ****p < 0.0001. n=3, number of rats.

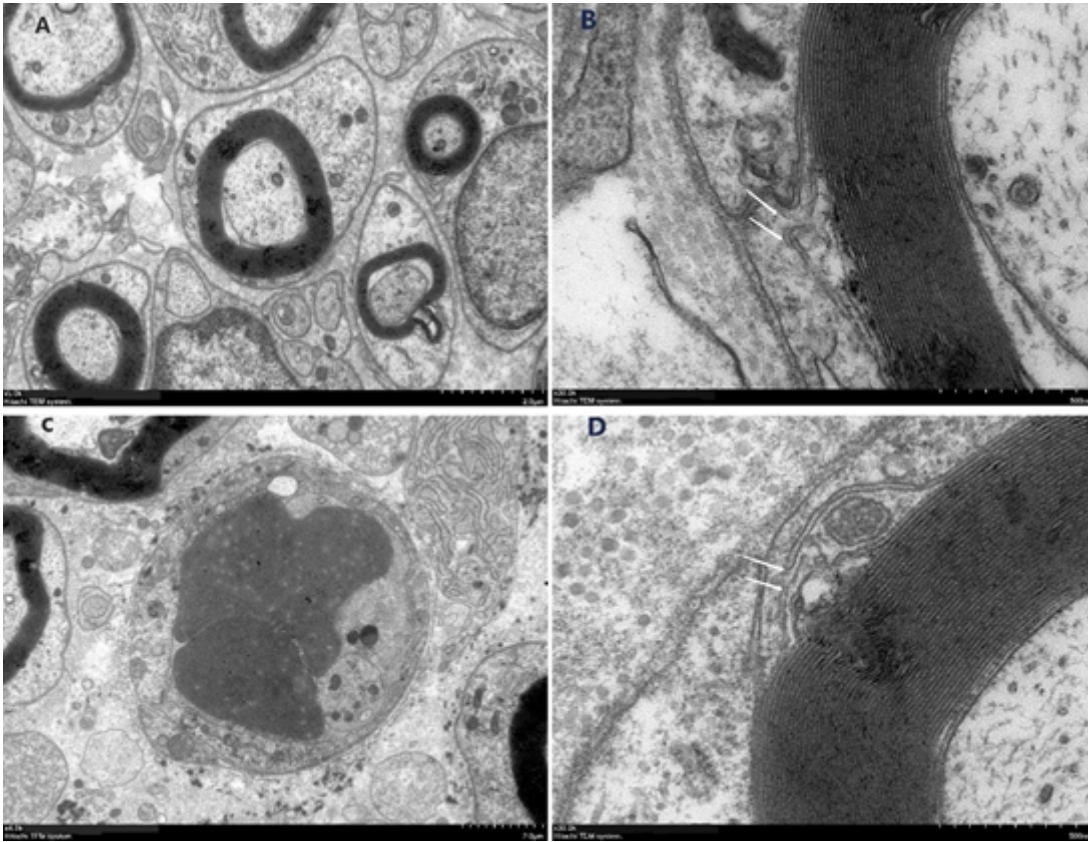


Figure 5

Transmission electron micrographs of (A,B) normal sciatic nerve segment and (C,D) sciatic nerve segment at 3 days after JEV infected. Arrows pointed to the kissing points of tight junctions. In A and C, magnifications were $\times 5.0$ k and $\times 4.0$ k, respectively, and the scale bar represented $2\mu\text{m}$. In B and D, magnification was $\times 30.0$ k and the scale bar represented 500 nm.

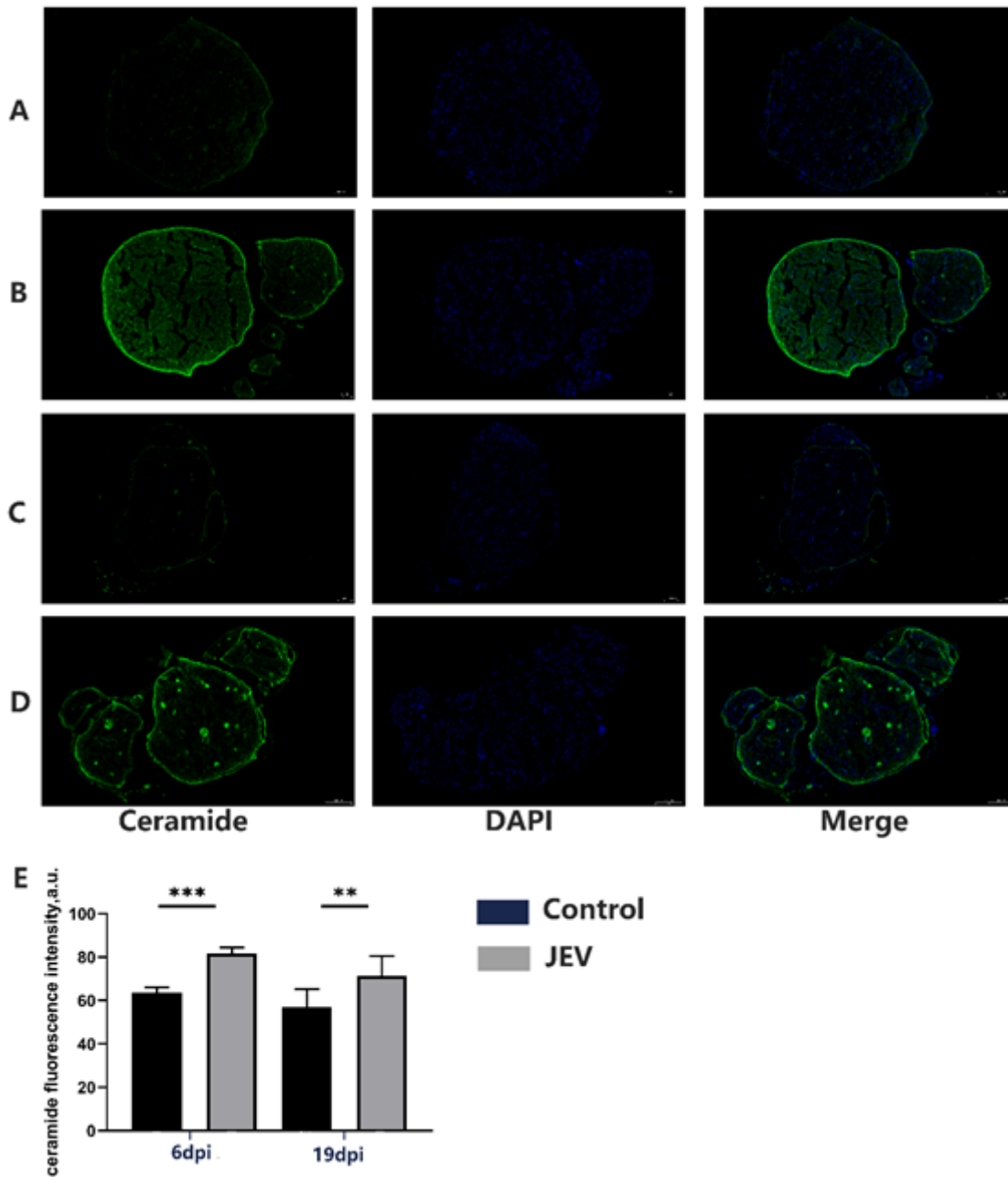


Figure 6

Ceramide increased in Sciatic nerve of JEV infected rat. Expression of ceramide (Cer) on transverse sections of Sciatic nerve fibers in control rats at 6dpi(A), rats after 6dpi of JEV infected (B) and in control rats at 19dpi (C). rats after 19dpi of JEV infected(D). Quantification of ceramide signal intensity after 6days and 19days(E). Scale bar-100 μ m. The graph is the quantification of ceramide fluorescence (mean \pm SEM). * $p < 0.05$; ** $p < 0.01$; *** $p < 0.001$; **** $p < 0.0001$ denote statistically significant differences in comparison with the control value; $n = 3$ rats for each group.

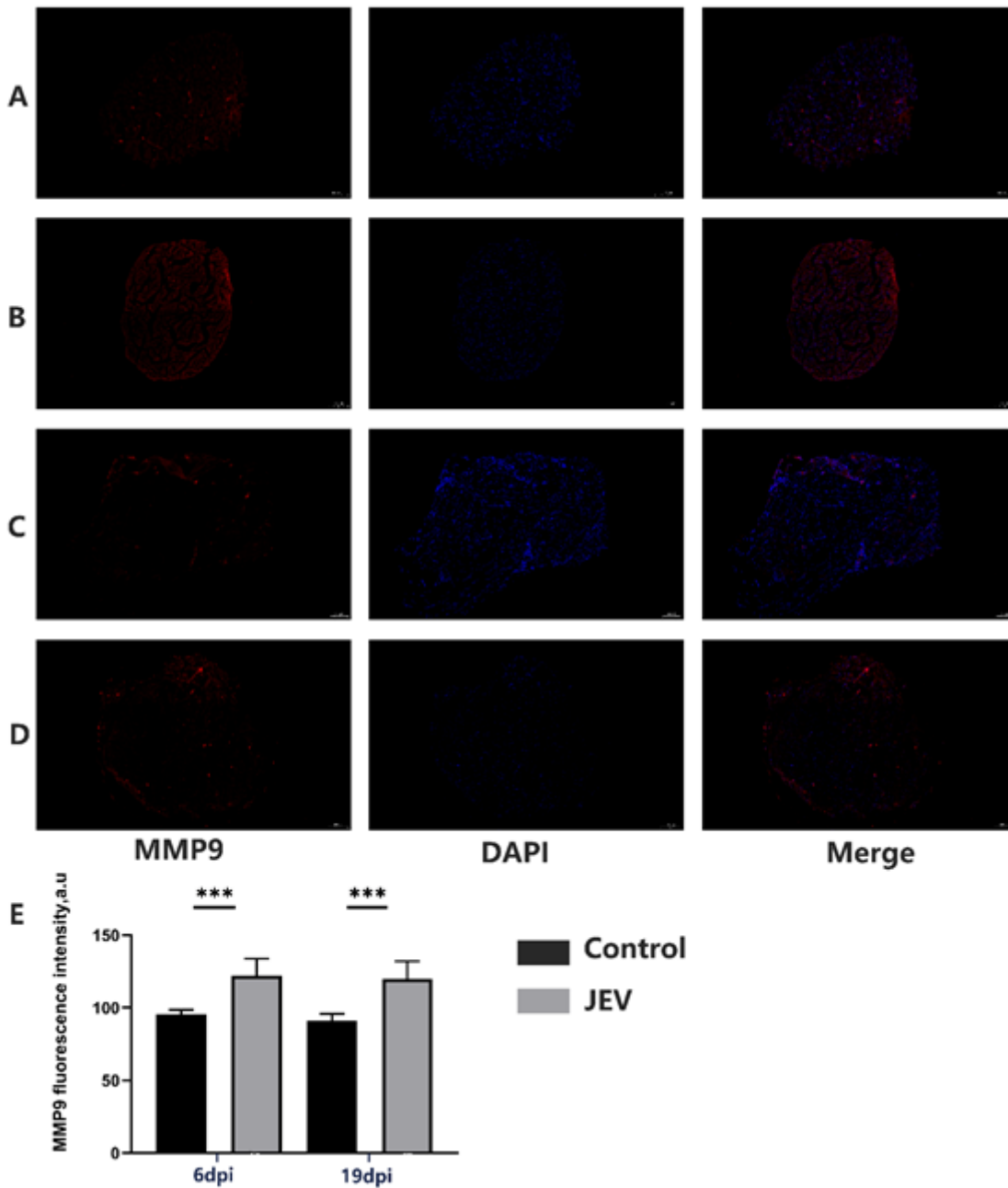


Figure 7

Matrix metalloproteinase-9 (MMP9) increased in Sciatic nerve of JEV infected rat. Expression of MMP9 on transverse sections of Sciatic nerve fibers in control rats at 6dpi (A), rats after 6dpi of JEV infected (B) and in control rats at 19dpi (C), rats after 19dpi of JEV infected (D). Quantification of MMP9 signal intensity after 6 days and 19 days (E). Scale bar-100 μ m. The graph is the quantification of MMP9 fluorescence (mean \pm SEM). * $p < 0.05$; ** $p < 0.01$; *** $p < 0.001$; **** $p < 0.0001$ denote statistically significant differences in comparison with the control value; $n = 3$ animals for each group.

Supplementary Files

This is a list of supplementary files associated with this preprint. Click to download.

- [weightscore.tif](#)